Characterization of the Proton-Transporting Photocycle of Pharaonis Halorhodopsin

Ágnes Kulcsár,* Géza I. Groma,* Janos K. Lanyi,† and György Váró*

*Institute of Biophysics, Biological Research Center of the Hungarian Academy of Sciences, Szeged, H-6701, Hungary; and †Department of Physiology & Biophysics, University of California, Irvine, California 92697 USA

ABSTRACT The photocycle of pharaonis halorhodopsin was investigated in the presence of 100 mM NaN_3 and 1 M Na_2SO_4. Recent observations established that the replacement of the chloride ion with azide transforms the photocycle from a chloride-transporting one into a proton-transporting one. Kinetic analysis proves that the photocycle is very similar to that of bacteriorhodopsin. After K and L, intermediate M appears, which is missing from the chloride-transporting photocycle. In this intermediate the retinal Schiff base deprotonates. The rise of M in halorhodopsin is in the microsecond range, but occurs later than in bacteriorhodopsin, and its decay is more accentuated multiphasic. Intermediate N cannot be detected, but a large amount of O accumulates. The multiphasic character of the last step of the photocycle could be explained by the existence of a HR′ state, as in the chloride photocycle. Upon replacement of chloride ion with azide, the fast electric signal changes its sign from positive to negative, and becomes similar to that detected in bacteriorhodopsin. The photocycle is enthalpy-driven, as is the chloride photocycle of halorhodopsin. These observations suggest that, while the basic charge translocation steps become identical to those in bacteriorhodopsin, the storage and utilization of energy during the photocycle remains unchanged by exchanging chloride with azide.

INTRODUCTION

Pharaonis halorhodopsin (pHR) is a small integral membrane protein in the haloalkaliphile *Natronobacterium pharaonis* (Bivin and Stoeckenius, 1986). It belongs to the family of retinal proteins, like bacteriorhodopsin (BR) and salinarum halorhodopsin (sHR) from *Halobacterium salinarum*. Upon photoexcitation it transports chloride ion into the cell (Duschl et al., 1990). Amino acid sequence comparison reveals a 25% homology of pHR with the proton transporter BR and 66% with the chloride transporter sHR (Lanyi et al., 1990). The extent of identity is greater in the putative seven transmembrane helices, and the residues in the retinal binding pocket are particularly highly conserved. The important exceptions are the proton acceptor Asp-85 and proton donor Asp-96 in BR, which are replaced by Thr and Ala, respectively, in both halorhodopsins. Lack of the proton acceptor ensures that the Schiff base remains protonated during the photocycle while chloride is transported through the membrane.

No structural information exists about pHR, but its sequential identity and functional similarity with sHR makes it probable that it has a similar structure, i.e., seven transmembrane helices surrounding the retinal binding pocket (Havelka et al., 1995). The retinal is bound to Lys-256 via a protonated Schiff base in all-*trans* or 13-*cis* configuration. Contrary to BR and sHR, its retinal isomer composition is independent of illumination, containing 85% all-*trans* and 15% 13-*cis* retinal (Váró et al., 1995a; Zimányi and Lanyi, 1997). Although the protein suspension is not homogeneous in retinal conformation, there is no evidence that the 13-*cis*-containing protein is photoactive (Váró et al., 1995a).

Spectral titration of pHR with sodium chloride yields a chloride-binding constant of 1 mM, characterized by a 13-nm blue shift of the absorption peak (Scharf and Engelhard, 1994; Váró et al., 1995a). Other halide ions also bind to the protein with similar spectral shifts but different binding constant (Scharf and Engelhard, 1994). Raman and FTIR spectroscopic studies proved the existence of an interaction between the retinal Schiff base and halide ion (Walter and Braiman, 1994; Gerscher et al., 1997). Titration with azide causes almost the same spectral change, with a binding constant of 10 mM, and chloride and azide ions compete for the same binding site (Váró et al., 1995a). In salt-free solution the protein denaturates. For this reason, during titration the sodium content of the solution is kept constant by supplementing the titrated salt with sodium sulfate, which itself does not bind to the protein (Scharf and Engelhard, 1994; Váró et al., 1995a).

Azide was used as a substitute for the proton donor in the study of the D96N BR mutant (Tittor et al. 1989; Zimányi and Lanyi, 1993). In several cases azide could also replace the role of the proton acceptor Asp-85 (Tittor et al., 1994; Dickopf et al., 1995). In wild type BR azide has an observable effect on the decay of intermediate M only at very high concentrations (Ormos et al., 1997). In sHR the presence of azide resulted a side-reaction of the photocycle, yielding deprotonation of the Schiff base (Hegemann et al., 1985). In pHR azide could replace both the proton donor and acceptor in chloride-free solution and lead to a proton transporting photocycle (Váró et al., 1996).

Received for publication 28 March 2000 and in final form 21 July 2000.

Address reprint requests to Dr. Gyorgy Varo, Institute of Biophysics, Biological Research Center of the Hungarian Academy of Sciences, Szeged, H-6701, Hungary. Tel.: 36-62-432232; Fax: 36-62-43331333; E-mail: varo@nucleus.szbk.u-szeged.hu.

0006-3495/00/11/2705/09 $2.00

The chloride-transporting photocycle of halorhodopsin has intermediates analogous to the BR photocycle, but without an M intermediate containing a deprotonated Schiff base (Váró et al., 1995a,b). The only important difference between the photocycle of the two halorhodopsins is that in the photocycle of sHR the intermediate O was not observed (Váró et al., 1995a), whereas in the photocycle of pHR this intermediate accumulates in rather large amounts (Váró et al., 1995b). In the photocycle of sHR the observed red-shifted species, which earlier was assigned as intermediate O, belongs to the non-transporting 13-*cis* photocycle (Váró et al., 1995a). There is no evidence to decide if intermediate O is really missing from the photocycle, or for kinetic reasons does not accumulate. Based on the multiexponential decay of the pHR photocycle, the HR′ state was introduced as the last intermediate, with essentially the same spectrum as HR (Váró et al., 1995a). When chloride is replaced with azide, the M intermediate appears in the photocycle of pHR (Váró et al., 1996). There are other conditions, when an M-like intermediate appears in the halorhodopsin photocycle, such as double flash excitation (Bamberg et al., 1993) or prolonged illumination (Hegemann et al. 1985), when both azide and chloride are present in the sample. These M-like intermediates have a very long lifetime and transport protons across the membrane only when the illumination is with both green and blue light. From the temperature dependence of the photocycle, the free energy, enthalpy and entropy changes of the reactions were determined. The pH dependence of the energetics of BR photocycle is complex, but the driving force of the reactions is mostly the entropy decrease (Ludmann et al., 1998b). In contrast, the photocycle reactions of pHR are enthalpy-driven (Váró et al., 1995b).

It has been suggested that there must be an analogy between proton transport in BR and chloride transport in HR (Oesterhelt and Tittor, 1989; Oesterhelt et al., 1992; Haupts et al., 1997; Brown et al., 1998; Váró, 2000). This implies the possibility that either protein could be converted to the ion specificity of the other. When Thr replaced the proton acceptor Asp-85, the function of BR changed from proton to chloride translocation (Sasaki et al., 1995). The same effect could be achieved by neutralizing the proton acceptor at low pH. The pK_a of Asp-85 is approximately 2.6 (Balashov et al., 1991; Balashov et al., 1995). At pH below 2, with chloride ion present, BR transports chloride through the membrane (Dér et al., 1989, 1991).

The electric response signal of a light activated protein can be measured on anisotropic sample consisting of oriented membranes. These electric signals reveal details about the ion-transporting steps in the photocycle. Oriented samples can be obtained by incorporating the protein containing membrane fragments into a bilayer lipid membrane (Bamberg et al., 1981, 1984), or by oriented attachment of purple membranes to a lipid-impregnated filter (Drachev et al., 1984) or thin Teflon films (Holz et al., 1988). Another possibility is to apply an external electric field to the membrane suspension (Keszthelyi and Ormos, 1983; Keszthelyi and Ormos, 1989). This orientation can be fixed if the membranes are polymerized in an acrylamide gel, when the external electric field is applied (Dér et al., 1985a,b). The measured photoelectric response signals show a strong correlation with the photocycle (Keszthelyi and Ormos, 1989). The electrogenicity of an intermediate (by definition the change of the electric dipole moment of the protein in that intermediate relative to the unexcited state) characterized the magnitude of the charge shifts inside the protein (Trissl, 1990). The sign of the electrogenicity was considered positive, when the change of the electric dipole corresponds to the shift of a positive charge toward the extracellular side of the membrane. The electrogenicity of the intermediates in the BR photocycle and in the chloride photocycle of pHR were determined (Ludmann et al., 1998a, 2000). These help understand the process of charge transfer through the membrane.

In the present work the photocycle of pHR was investigated in the presence of azide and absence of chloride. The replacement of chloride ion with azide makes possible the deprotonation of the Schiff base, resulting in an M-like intermediate. Measurements on cell envelope vesicles proved that proton is transported through the membrane (Váró et al., 1996). Time-resolved spectroscopic, absorption kinetic and electric signal measurements could reveal details about the changes of the photocycle. Using time-resolved spectroscopy the spectra of photocycle intermediates can be determined (Nagle et al., 1995; Gergely et al., 1997; Zimányi et al., 1999). Absorption kinetic measurements at several wavelengths help to determine the photocycle model and calculate the microscopic rate constants (Váró et al., 1995b; Ludmann et al., 1998b). By electric signal measurements the charge motions inside the protein can be studied, which give information about the motion of the transported ion through the membrane (Ludmann et al., 1998a, 2000; Dér et al., 1999). Applying all these techniques, the similarities and differences between the azide photocycle of pHR and that of BR were investigated.

MATERIALS AND METHODS

Halorhodopsin-containing membrane suspension was prepared from *Halobacterium salinarum* strain L33, in which the *Natronobacterium pharaonis hop* structural gene and the novobiocin resistance gene for selection were introduced. This resulted in a greatly enhanced production of pHR. The process of preparation of the suspension was described earlier (Váró et al., 1995a). All spectroscopic and absorption kinetic measurements were performed on membranes encased in polyacrylamide gels, as described before (Váró et al., 1995c) on a sample of optical density about 1 at 570 nm. Electric signal measurements were carried out on oriented gel samples, prepared according to the procedure described earlier (Dér et al., 1985b). Before measurements the samples were exhaustively washed in a solution of 1 M Na_2SO_4, 50 mM (2-[*N*-morpholino]ethanesulfonic acid) MES, 100 mM NaN_3, pH 6. In the case of electric signal measurement, the concentration of Na_2SO_4 and MES was reduced to half to lower the

conductivity of the sample. This change in the salt concentrations did not introduce any observable alteration in the kinetics.

Laser excitation was performed with a frequency-doubled Nd-YAG laser (Continuum, Surelite I-10, $\lambda = 532$ nm). During the measurement the sample was kept in a temperature-controlled sample holder. Time-resolved spectroscopy with a gated optical multichannel analyzer provided difference spectra at various time points of the photocycle (Zimányi et al., 1989). The spectra of intermediates were calculated from these difference spectra, after noise reduction with singular value decomposition (SVD) (Golub and Kahan, 1992; Váró and Lanyi, 1991; Gergely et al., 1997). Absorption kinetic signals were recorded at five wavelengths (410, 500, 570, 610, and 650 nm) and five temperatures between 10 and 30°C, in a time interval from 100 ns to 1 s, using a transient recorder card with 16 MB memory (National Instruments, NI-DAQ PCI-5102), controlled by a program developed in our Institute. Each measurement involved averaging of 100–200 signals. At the end of the measurement, the linear time base was converted to a logarithmic one by averaging in the time interval between logarithmically equidistant points, which improved the signal to noise ratio. Model fitting was performed with the RATE program, as described elsewhere (Ludmann et al., 1998b). From the temperature dependence of the rate constants the energetic picture of the reactions were calculated, using the EYRING program (Ludmann et al., 1998b). Electric signals were measured on the earlier described set-up (Gergely et al., 1993), with the modification that a very low-noise home-made amplifier was used. The time resolution of the system was about 100 ns.

RESULTS

The replacement of the 1 M NaCl with 100 mM NaN_3 and 1 M Na_2SO_4 produces dramatic changes in the absorption kinetic signals (Fig. 1, *A* and *B*). The most important change is the absorption increase at 410 nm, characteristic of the intermediate M containing deprotonated Schiff base. In the presence of chloride ion the dominant absorption maximum was at 500 nm, which characterizes the L intermediate that persists over the entire photocycle (Fig. 1 *A*). In azide the absorption at 500 nm has a maximum at around 10 μs and later decreases to negative values (Fig. 1 *B*). This implies that in the photocycle with azide the intermediate L disappears in the millisecond range. The absorption kinetic signals measured at five wavelengths are very similar to that measured on BR (Fig. 1 *C*). The resemblance of the kinetic traces measured in pHR with azide and BR suggests that the photocycles are similar. To analyze the similarities and differences a thorough study was carried out, as described below.

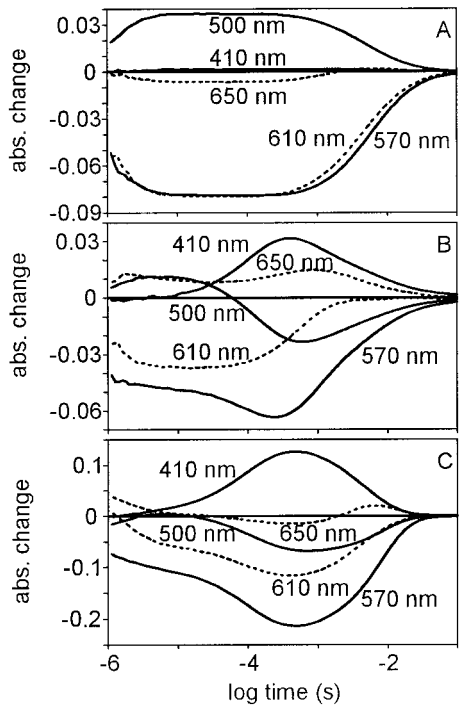

FIGURE 1 Absorption kinetic signals measured at five wavelengths on pharaonis halorhodopsin (*A*) and bacteriorhodopsin (*C*) in 1 M NaCl, 50 mM MES, pH 6, 20°C, and on pharaonis halorhodopsin (*B*) in 100 mM NaN_3, 1 M Na_2SO_4, 50 mM MES, pH 6, 20°C.

The difference spectra measured with an optical multichannel analyzer were submitted to SVD analysis. The autocorrelation function of the basis spectra and their time dependence showed a long-range structure in the first four components. The other components contained only noise. The weight factors of the four components were 83.6, 36.2, 16.4, and 2.2. All the following weight factors were much smaller. The analysis therefore suggests the existence of at least four independent spectral components. Noise-filtered difference spectra were reconstructed from these four SVD components (Fig. 2) and used in the calculation of the spectra of the intermediates. The difference spectra taken at the early time points show the existence of a red-shifted component around 650 nm, presumably the K intermediate. Later a peak around 500 nm appears, which can be attributed to intermediate L. Its decay is accompanied by the appearance of a strongly blue-shifted peak at around 410 nm, characteristic of intermediate M. The red-shifted peak does not disappear completely, but when the absorption at 410 nm approaches its maximum, a downshift of the red part of the difference spectrum can be observed, accompanied by an absorption increase, which suggests the appearance of another intermediate. Finally all the absorption changes disappear, showing that the pHR returns to its unexcited state.

Because the intermediates strongly overlap both spectrally and in time, finding a unique set of spectra is seriously hampered (Gergely et al., 1997). A control in the process of calculation was a reasonable model fit with RATE to the five absorption kinetic signals, when the extinction coefficients of the intermediates were taken from the calculated spectra. Based on the kinetic similarities between the studied photocycle and that belonging to BR (Fig. 1, *B* and *C*), the search was started with the same number of intermediates and with a model containing reversible reactions. When five intermediate spectra were calculated (K, L, M, N, and O; data not shown) the spectrum of N was very broad and its peak coincided with that of HR. No matter how the starting parameters of the fit to the absorption kinetic signals were taken, the fitting procedure resulted in no N

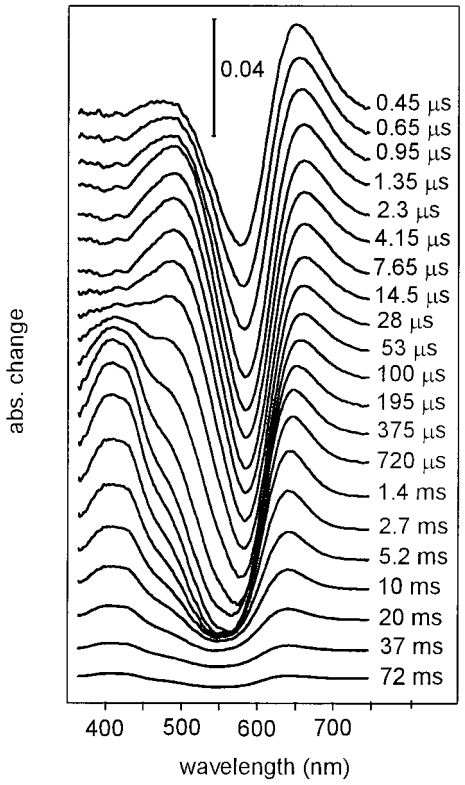

FIGURE 2 SVD-filtered, time-resolved difference spectra measured on pharaonis halorhodopsin at the indicated times after the photoexcitation. Measuring conditions: 1M Na_2SO_4, 100 mM NaN_3, 50 mM MES, pH 6 and 20°C.

intermediate in the photocycle. This led us to the conclusion that only the spectra of K, L, M, and O intermediates are present in the set of difference spectra. Using this information the spectra of the intermediates were calculated (Fig. 3).

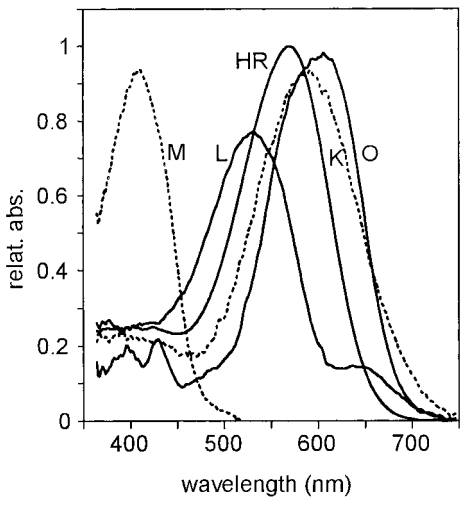

FIGURE 3 The spectra of intermediates calculated from the difference spectra shown in Fig. 2. The small secondary peak in the spectrum of L can be attributed to the 5–10% sulfate photocycle present after the photoexcitation.

Based on the resemblance of the azide photocycle with that of BR, but with a multiphasic decaying part (similar to pHR) and no intermediate N, the initially considered model was:

$$K \Leftrightarrow L \Leftrightarrow M \Leftrightarrow O \Leftrightarrow HR' \Rightarrow HR$$

Although the fit to the absorption kinetic signals (Fig. 4 *A*) had a relatively large error (±10%), it gave a general scheme about the time course of the concentrations of the intermediates (Fig. 4 *B*). The error could be attributed to the above-mentioned presence of the sulfate photocycle. In the starting model all the transitions were reversible, except the last one, ensuring that the photocycle terminates in a stable product. The fit resulted an M to L back-transition infinitely slow, leading to a model with a unidirectional step between these two intermediates:

$$K \Leftrightarrow L \Rightarrow M \Leftrightarrow O \Leftrightarrow HR' \Rightarrow HR$$

This results in the disappearance of intermediates K and L in the second part of the photocycle. Large amount of O appears, in strong equilibrium with intermediate M, which does not accumulate as much as in BR. The HR′ intermediate had to be considered, based on the very long, multiexponential decay of the absorption kinetic signals, and introduced earlier for a similar reason in the chloride photocycle

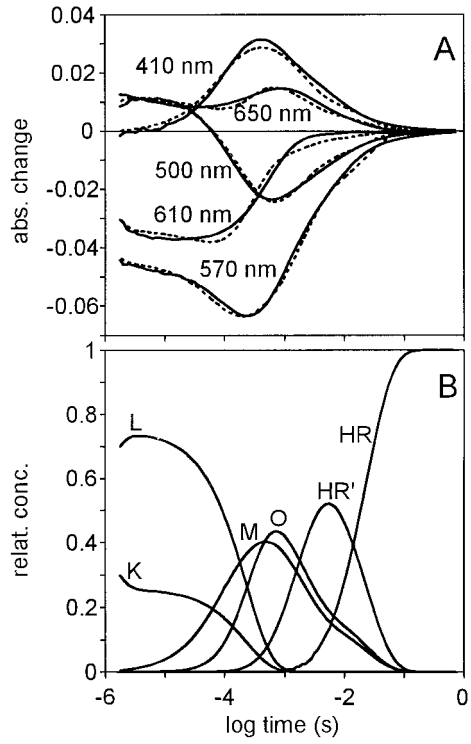

FIGURE 4 (*A*) the fit of the photocycle model (*broken lines*) to the absorption kinetic signals (*continuous lines*). (*B*) time evolution of the concentration of the intermediates. Measuring conditions were the same as in Fig. 2. The error of the fit was ±10%.

of pHR (Váró et al., 1995a,b). To determine the energetic scheme of the photocycle, the temperature dependence of the absorption kinetic signals were measured between 10°C and 30°C (Fig. 5). Below 10°C it was impossible to make this measurement: the Na_2SO_4 precipitated, and the sample became opaque and scattered the measuring light. Despite the large error in the model fit, the Eyring plot of the rate constants showed a reasonable linear dependence (Fig. 6), indicating that the model is correct.

The fit of the data with two parallel photocycles was also investigated. The temperature dependence of the rate constants gave no linear Eyring plot, eliminating this model from further consideration, similar to the case described earlier for BR (Ludmann et al., 1998b).

The free energy, enthalpy, and entropy of the photocycle transitions were calculated as previously (Váró et al., 1995a; Ludmann et al., 1998b) using the Eyring formula:

$$\ln k = -\frac{\Delta H^*}{R \cdot T} + \frac{\Delta S^*}{R} + \ln\frac{k_B \cdot T}{h}$$

$$\Delta G^* = \Delta H^* - T \cdot \Delta S^*$$

where k is the rate constant, T is the temperature expressed in °K, R is the gas constant, k_B is the Boltzmann constant, and h is the Planck's constant. From the calculated transition energies the energetic scheme of the whole photocycle was drawn (Fig. 7). All the energy levels are relative to K (or M in the second part). The exact position of the energy level of K (or M), relative to unexcited HR is not known, because the quantum efficiency and the energy stored in K were not determined. As the reverse transition M to L does not exist (it is unmeasurably slow, compared to the others), all that is known is that the free energy level of M is much lower than that of L, but no information exists about its position in enthalpy and entropy diagrams. Although M is placed at the same level as K, the dashed line separates the two parts, indicating that they are not related. The enthalpy and entropy diagrams show great similarity to that of chloride transporting pHR (Váró et al., 1995b).

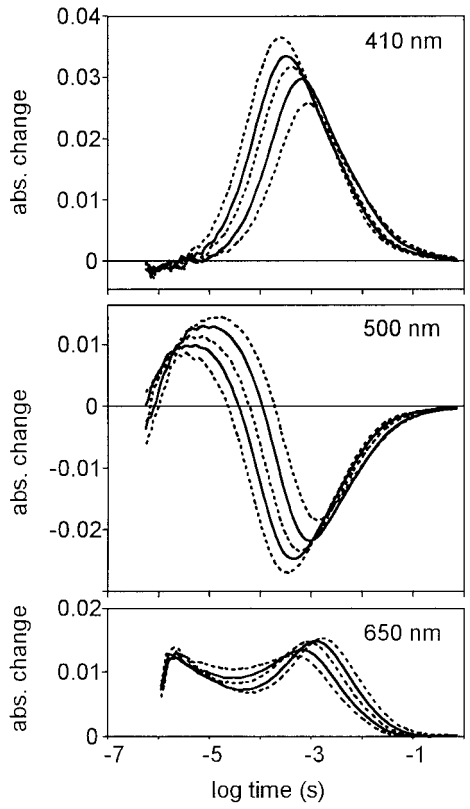

FIGURE 5 Absorption kinetic signals measured on pharaonis halorhodopsin at different temperatures. From right to left the temperatures are 10, 15, 20, 25, and 30°C. The other measuring conditions were the same as in Fig. 2.

The light-induced electric response signal measurements provide information about the charge motions inside the membrane. The electric signals of pHR were much smaller than that of BR. The membranes containing pHR form almost closed vesicles leading to a low degree of orientation by external electric field applied in the course of the sample preparation. The samples were measured in three different bathing solutions and compared with each other and with that of BR (Fig. 8). The fast component of the current signal measured in the presence of chloride is positive (in the same direction as that of the net charge transport) (curve A), in sulfate is negative (curve B), whereas in azide it is negative and crosses the zero line (curve C), becoming very similar to that of BR (curve BR).

DISCUSSION

The changes in the absorption kinetic signals when the chloride is exchanged with azide (Fig. 1) and the resemblance of these traces to that of BR raises the following questions: What kind of processes inside the protein were changed? Which steps are common in the proton and chloride translocation and which are different? Which steps determine the specificity of the transported ion? To clarify these questions, a thorough investigation of the azide pumping photocycle of pHR was carried out and compared to the two related photocycles: the proton transporting photocycle of the BR and the chloride transporting photocycle of the pHR.

It was established before that the binding constant of azide to pHR is 10 mM (Váró et al., 1996). In the bathing solution of the sample 1 M Na_2SO_4 and 100 mM azide was present, leading to a non-homogeneous sample containing 90–95% azide-bound protein. Because the spectrum of the azide-free protein is shifted with about 13 nm toward the red, the laser excitation at 532 nm is less effective upon it than upon the azide-bound pHR. Maximum 10% of the excited protein goes through the so-called sulfate photocycle (Váró et al., 1995a). This photocycle consists of only one intermediate, with its absorption maximum around 670

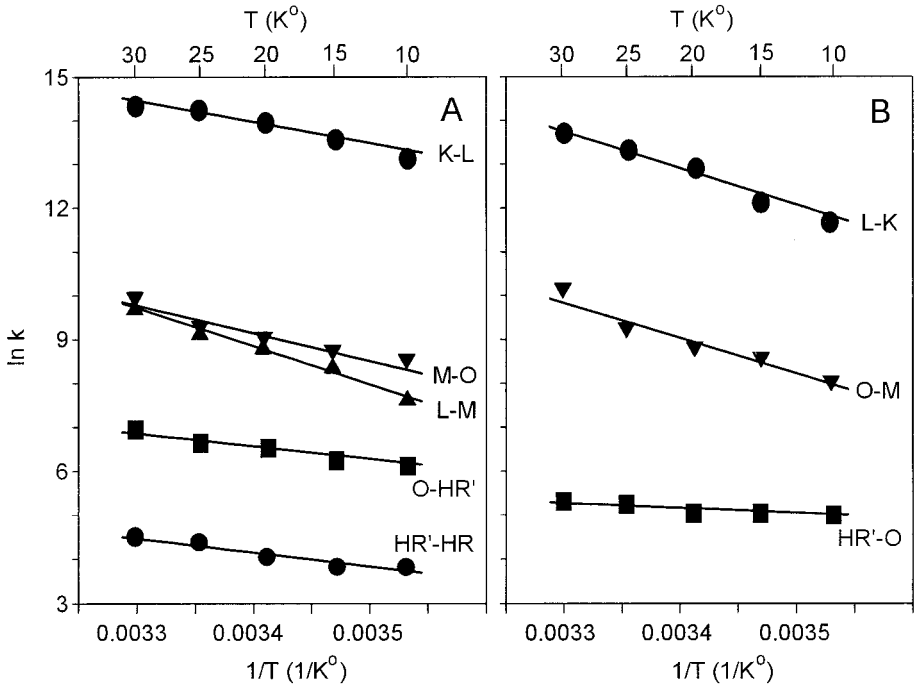

FIGURE 6 The Eyring diagram of the rate constants calculated from the model with reversible reactions. The lines are the fits from which the thermodynamic parameters were calculated. (*A*) Forward reactions of the model. (*B*) Back reactions. The error of the fit is ±5%.

nm, and decays in the 10 μs to millisecond time domain. The broadening in the red side of the spectrum of intermediate K and the small extra peak in L (Fig. 3) were attributed to this photocycle. Not having exact information about the quantum efficiencies of the two protein forms, which contribute to the signal, it would be very difficult to separate the two photocycles. The 10% sulfate photocycle is considered as an error in the fitting procedure, when the extinction coefficients are taken from the spectra of intermediates at

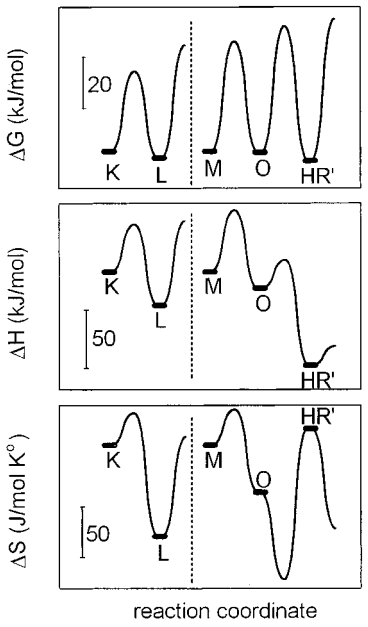

FIGURE 7 The free energy, enthalpy, and entropy diagram of the pharaonis halorhodopsin azide photocycle calculated form the fits shown in Fig. 6. The transition between intermediates L and M is unidirectional, which leaves undetermined the position of the energy level corresponding to M, represented by the separating broken lines between the two intermediates.

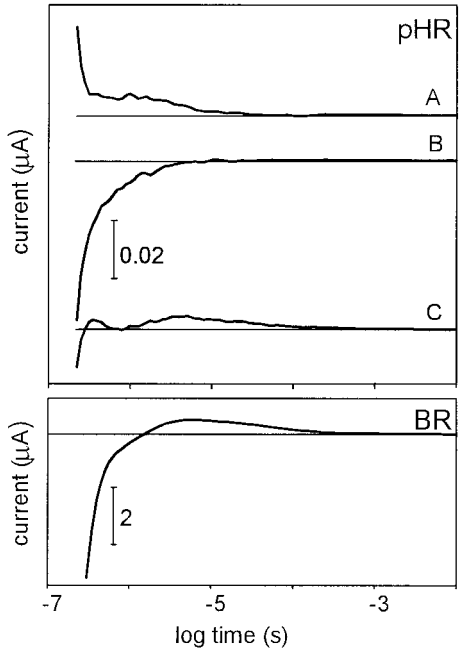

FIGURE 8 Light-induced electric signals of pharaonis halorhodopsin (*upper panel*) and bacteriorhodopsin (*lower panel*) measured on oriented gel samples. The measuring conditions are as follows: Line A and BR were measured in 1M NaCl, line B in 0.5 M Na_2SO_4, and line C in 0.5 M Na_2SO_4 and 100 mM NaN_3. All solutions had 25 mM MES, pH 6, 20°C.

the measured wavelengths. It is known that the sulfate photocycle is completed in several ms and affects only the red end of the intermediate spectra. Nevertheless, when the absorption kinetic traces are fitted with the RATE program, the errors are distributed uniformly on all wavelengths (Fig. 4 *A*).

The time-dependent concentration changes of the intermediates of the azide photocycle of pHR were compared (Fig. 4 *B*) with the chloride photocycle (Váró et al., 1995a) and that of BR photocycle (Ludmann et al., 1998b). The K to L transition is as fast as in chloride, but the equilibrium between the two intermediates is shifted to a lower K concentration and these intermediates disappear from the photocycle in the ms time region, similar to that in BR. In the microsecond range, but later than in BR, the M intermediate appears, indicating that the Schiff base deprotonates. The rise of M is not as clearly multiphasic as in BR. The model fit did not demand the introduction of two M forms, but this does not exclude the existence of them. In both BR and pHR, intermediate M reaches its maximum concentration in about the same time. The elimination of intermediate N from the photocycle model does not mean that it is completely excluded, only that it can not be observed. Our measurements can not decide, whether N is absent from this photocycle or only due to kinetic reasons does not accumulate. Instead of N a large amount of O is accumulated. The equilibrium constant of the M to O transition is almost 1, resulting in a equal amount of intermediates M and O, decaying through HR′ to HR.

All the transitions in the second part of the photocycle have weak temperature dependence, reflected in the absorption kinetic measurements over the millisecond time range (Fig. 5). The only exception is in the 650 nm measurement, characteristic for intermediate O, where a more accentuated change can be observed. With increasing temperature the amount of intermediate O decreases, contrary to the BR photocycle (Fig. 5, panel 650 nm). This can be attributed to the fact that the slope of the reverse transition O to M is larger than that corresponding to M to O and all the other transitions after intermediate O (Fig. 6). The free energy scheme, calculated from the Eyring plots, show two unidirectional reactions, between intermediates L and M, and the final decay of HR′. A reaction between two intermediates was considered unidirectional, when the forward reaction is at least 100 times faster than the corresponding back reaction. This corresponds to at least −11 kJ/mol free energy difference between the two states. The BR photocycle measured over pH 6 had also two unidirectional reactions (Ludmann et al., 1998b). The free energy scheme of both chloride transporting photocycle of pHR and the proton-transporting photocycle of BR are similar. Great differences exist in the enthalpy and entropy changes, however. While the reactions in the photocycle of BR are entropy-driven, because the entropic energy ($-T\Delta S$) decreases in almost every reaction (Ludmann et al., 1998b), the transitions in the chloride photocycle of pHR are enthalpy-driven (Váró et al., 1995a). The transitions in the azide photocycle of pHR are also enthalpy-driven. Except the reaction between intermediates L and M, where there is no information about the relation between the energy levels, all the other enthalpy levels look very similar to the chloride photocycle. The change in the function of the protein did not change the way the energy is stored and used during the photocycle. From the thermodynamic study can be concluded that in BR the conformational changes of the protein drive the photocycle, resulting in decreasing entropy. In pHR the driving force results mainly from changes in the electrostatic interactions inside the protein.

The electric signals are characteristic to the charge translocation steps in BR and pHR (Ludmann et al., 1998a, 2000). The fast component of the current signal in BR and pHR in different conditions were compared (Fig. 8). In BR the electrogenicity of intermediate K was negative, the L also negative and about two times larger, resulting in a fast negative signal, which crosses the zero line, becoming positive in several microseconds (Fig. 8, BR). The positive current corresponds to the rise of the M intermediate (Ludmann et al., 1998a). In the chloride photocycle of pHR the electrogenicity of K was negative, that corresponding to L was positive and about three times larger, resulting in a positive signal (Fig. 8 *A*) (Kalaidzidis et al., 1998; Ludmann et al., 2000). With pHR in sulfate, where a K-like intermediate dominates the photocycle (Váró et al., 1995a), the fast component was negative and it decayed to zero, without any positive component (Fig. 8 *B*) (Ludmann et al. 2000). When azide was added, the fast component of the current signal was also negative and later crossed the zero line (Fig. 8 *C*). As the electric signal was very small, and the fast component was close to the time resolution of the systems (100 ns), it cannot be excluded that the first positive peak is an overshoot, after the negative component. The second positive peak, in the microsecond time domain, corresponds to the rise of the intermediate M. The appearance of the fast negative component and the positive component corresponding to intermediate M makes the photoelectric response signal of the azide photocycle very similar to that of BR (Fig. 8).

The combination of electrogenicities corresponding to intermediates K and L yields the fast part of the electric response signal. Depending on their sign and amplitude, the result can be either positive or negative. The K intermediate, which corresponds to the retinal isomerization in all photocycles, has negative electrogenicity (Ludmann et al., 1998a; Ludmann et al. 2000). This process seems to be similar in both proteins at all conditions. The electric signal of the L intermediate corresponds to a local relaxation of the protein around the retinal chromophore. This relaxation is sensitive to the presence of the proton acceptor. It is positive in the absence of the proton acceptor and decreases or becomes

negative when the acceptor is present. All the other transporting steps are positive (Ludmann et al., 1998a, 2000).

Comparing the proton-transporting photocycle of pHR in the presence of azide to that of BR, it is shown here that kinetically they are very similar, with the very characteristic intermediate M containing unprotonated Schiff base. The process of charge translocation, manifested in the electric signal, is also very similar in the azide photocycle of pHR and BR. On the other hand, energetically the azide photocycle remains analogous to that of the chloride transporting one. It is driven by enthalpy decrease during the transitions between the intermediates. The transformation of the chloride-transporting photocycle to the proton-transporting one by simply replacing chloride with azide, which takes the role of both the proton donor and acceptor in the protein and the great similarity of it to that of BR, proves that the two very different ions are transported via the same basic steps.

We are grateful to Prof. L. Keszthelyi and Dr. L. Zimányi for helpful discussions. This work was supported by grants from the National Science Research Fund of Hungary (OTKA T022066, T020470) and the Research Fund of the Hungarian Academy of Sciences (AKP 97–71 3, 3/52).

REFERENCES

Balashov, S. P., R. Govindjee, and T. G. Ebrey. 1991. Red shift of the purple membrane absorption band and the deprotonation of tyrosine residues at high pH: origin of the parallel photocycles of trans-bacteriorhodopsin. *Biophys. J.* 60:475–490.

Balashov, S. P., R. Govindjee, E. S. Imasheva, S. Misra, T. G. Ebrey, Y. Feng, R. K. Crouch, and D. R. Menick. 1995. The two pK_a's of aspartate-85 and control of thermal isomerization and proton release in the arginine-82 to lysine mutant of bacteriorhodopsin. *Biochemistry.* 34:8820–8834.

Bamberg, E., N. A. Dencher, A. Fahr, and M. P. Heyn. 1981. Transmembranous incorporation of photoelectrically active bacteriorhodopsin in planar lipid bilayers. *Proc. Natl. Acad. Sci. USA.* 78:7502–7506.

Bamberg, E., P. Hegemann, and D. Oesterhelt. 1984. Reconstitution of the light-driven electrogenic ion pump halorhodopsin into black lipid membranes. *Biochim. Biophys. Acta.* 773:53–60.

Bamberg, E., J. Tittor, and D. Oesterhelt. 1993. Light-driven proton or chloride pumping by halorhodopsin. *Proc. Natl. Acad. Sci. USA.* 90: 639–643.

Bivin, D. B., and W. Stoeckenius. 1986. Photoactive retinal pigments in haloalkalophilic bacteria. *J. Gen. Microbiol.* 132:2167–2177.

Brown, L. S., A. K. Dioumaev, R. Needleman, and J. K. Lanyi. 1998. Local-access model for proton transfer in bacteriorhodopsin. *Biochemistry.* 37:3982–3993.

Dér, A., K. Fendler, L. Keszthelyi, and E. Bamberg. 1985a. Primary charge separation in halorhodopsin. *FEBS Lett.* 187:233–236.

Dér, A., P. Hargittai, and J. Simon. 1985b. Time-resolved photoelectric and absorption signals from oriented purple membranes immobilized in gel. *J. Biochem. Biophys. Methods.* 10(5–6):295–300.

Dér, A., L. Oroszi, A. Kulcsár, L. Zimányi, R. Tóth-Boconádi, L. Keszthelyi, W. Stoeckenius, and P. Ormos. 1999. Interpretation of the spatial charge displacements in bacteriorhodopsin in terms of structural changes during the photocycle. *Proc. Natl. Acad. Sci. USA.* 96:2776–2781.

Dér, A., S. Száraz, R. Tóth-Boconádi, Z. Tokaji, L. Keszthelyi, and W. Stoeckenius. 1991. Alternative translocation of protons and halide ions by bacteriorhodopsin. *Proc. Natl. Acad. Sci. USA.* 88:4751–4755.

Dér, A., R. Tóth-Boconádi, and L. Keszthelyi. 1989. Bacteriorhodopsin as a possible chloride pump. *FEBS Lett.* 259:24–26.

Dickopf, S., U. Alexiev, M. P. Krebs, H. Otto, R. Mollaaghababa, H. G. Khorana, and M. P. Heyn. 1995. Proton transport by a bacteriorhodopsin mutant aspartic acid-85–>asparagine, initiated in the unprotonated Schiff base state. *Proc. Natl. Acad. Sci. USA.* 92:11519–11523.

Drachev, L. A., A. D. Kaulen, and V. P. Skulachev. 1984. Correlation of photochemical cycle, H+ release and uptake, and electrical events in bacteriorhodopsin. *FEBS Lett.* 178:331–335.

Duschl, A., J. K. Lanyi, and L. Zimányi. 1990. Properties and photochemistry of a halorhodopsin from the haloalkalophile, Natronobacterium pharaonis. *J. Biol. Chem.* 265:1261–1267.

Gergely, C., C. Ganea, G. I. Groma, and G. Váró. 1993. Study of the photocycle and charge motions of the bacteriorhodopsin mutant D96N. *Biophys. J.* 65:2478–2483.

Gergely, C., L. Zimányi, and G. Váró. 1997. Bacteriorhodopsin intermediate spectra determined over a wide pH range. *J. Phys. Chem. B.* 101:9390–9395.

Gerscher, S., M. Mylrajan, P. Hildebrandt, M. H. Baron, R. Müller, and M. Engelhard. 1997. Chromophore-anion interactions in halorhodopsin from *Natronobacterium pharaonis* probed by time-resolved resonance Raman spectroscopy. *Biochemistry.* 36:11012–11020.

Golub, G., and W. Kahan. 1992. Calculating the singular values and pseudo-inverse of a matrix. *SIAM J. Num. Anal.* 2:205–224.

Haupts, U., J. Tittor, E. Bamberg, and D. Oesterhelt. 1997. General concept for ion translocation by halobacterial retinal proteins: the isomerization/switch/transfer (IST) model. *Biochemistry.* 36:2–7.

Havelka, W. A., R. Henderson, and D. Oesterhelt. 1995. Three-dimensional structure of halorhodopsin at 7 Å resolution. *J. Mol. Biol.* 247:726–738.

Hegemann, P., D. Oesterhelt, and M. Steiner. 1985. The photocycle of the chloride pump halorhodopsin. I. Azide catalyzed deprotonation of the chromophore is a side reaction of photocycle intermediates inactivating the pump. *EMBO J.* 4:2347–2350.

Holz, M., M. Lindau, and M. P. Heyn. 1988. Distributed kinetics of the charge movements in bacteriorhodopsin: evidence for conformational substates. *Biophys. J.* 53:623–633.

Kalaidzidis, IV, Y. L. Kalaidzidis, and A. D. Kaulen. 1998. Flash-induced voltage changes in halorhodopsin from *Natronobacterium pharaonis. FEBS Lett.* 427:59–63.

Keszthelyi, L., and P. Ormos. 1983. Displacement current on purple membrane fragments oriented in a suspension. *Biophys. Chem.* 18: 397–405.

Keszthelyi, L., and P. Ormos. 1989. Protein electric response signals from dielectrically polarized systems. *J. Membr. Biol.* 109:193–200.

Lanyi, J. K., A. Duschl, G. W. Hatfield, K. M. May, and D. Oesterhelt. 1990. The primary structure of a halorhodopsin from Natronobacterium pharaonis: structural, functional and evolutionary implications for bacterial rhodopsins and halorhodopsins. *J. Biol. Chem.* 265:1253–1260.

Ludmann, K., C. Gergely, A. Dér, and G. Váró. 1998a. Electric signals during the bacteriorhodopsin photocycle, determined over a wide pH range. *Biophys. J.* 75:3120–3126.

Ludmann, K., C. Gergely, and G. Váró. 1998b. Kinetic and thermodynamic study of the bacteriorhodopsin photocycle over a wide pH range. *Biophys. J.* 75:3110–3119.

Ludmann, K., G. Ibron, J. K. Lanyi, and G. Váró. 2000. Charge motions during the photocycle of pharaonis halorhodopsin. *Biophys. J.* 78: 959–966.

Nagle, J. F., L. Zimányi, and J. K. Lanyi. 1995. Testing BR photocycle kinetics. *Biophys. J.* 68:1490–1499.

Oesterhelt, D., and J. Tittor. 1989. Two pumps, one principle: light-driven ion transport in halobacteria. *Trends Biochem. Sci.* 14:57–61.

Oesterhelt, D., J. Tittor, and E. Bamberg. 1992. A unifying concept for ion translocation by retinal proteins. *J. Bioenerg. Biomembr.* 24:181–191.

Ormos, P., C. Gergely, S. Kruska, S. Száraz, and Z. Tokaji. 1997. The effect of azide on the photocycle of bacteriorhodopsin. *J. Photochem. Photobiol. B Biol.* 40:111–119.

Sasaki, J., L. S. Brown, Y.-S. Chon, H. Kandori, A. Maeda, R. Needleman, and J. K. Lanyi. 1995. Conversion of bacteriorhodopsin into a chloride ion pump. *Science.* 269:73–75.

Scharf, B., and M. Engelhard. 1994. Blue halorhodopsin from *Natronobacterium pharaonis*: wavelength regulation by anions. *Biochemistry.* 33: 6387–6393.

Tittor, J., C. Soell, D. Oesterhelt, H.-J. Butt, and E. Bamberg. 1989. A defective proton pump, point-mutated bacteriorhodopsin Asp96–>Asn is fully reactivated by azide. *EMBO J.* 8:3477–3482.

Tittor, J., M. Wahl, U. Schweiger, and D. Oesterhelt. 1994. Specific acceleration of de- and reprotonation steps by azide in mutated bacteriorhodopsins. *Biochim. Biophys. Acta.* 1187:191–197.

Trissl, H. W. 1990. Photoelectric measurements of purple membranes. *Photochem. Photobiol.* 51:793–818.

Váró, G. 2000. Analogies between halorhodopsin and bacteriorhodopsin. *Biochim. Biophys. Acta.* 1460:220–229.

Váró, G., L. S. Brown, R. Needleman, and J. K. Lanyi. 1996. Proton transport by halorhodopsin. *Biochemistry.* 35:6604–6611.

Váró, G., L. S. Brown, N. Sasaki, H. Kandori, A. Maeda, R. Needleman, and J. K. Lanyi. 1995a. Light-driven chloride ion transport by halorhodopsin from *Natronobacterium pharaonis.* 1. The photochemical Cycle. *Biochemistry.* 34:14490–14499.

Váró, G., and J. K. Lanyi. 1991. Kinetic and spectroscopic evidence for an irreversible step between deprotonation and reprotonation of the Schiff base in the bacteriorhodopsin photocycle. *Biochemistry.* 30:5008–5015.

Váró, G., R. Needleman, and J. K. Lanyi. 1995b. Light-driven chloride ion transport by Halorhodopsin from *Natronobacterium pharaonis*. 2. Chloride release and uptake, protein conformation change, and thermodynamics. *Biochemistry.* 34:14500–14507.

Váró, G., L. Zimányi, X. Fan, L. Sun, R. Needleman, and J. K. Lanyi. 1995c. Photocycle of halorhodopsin from *Halobacterium salinarium. Biophys. J.* 68:2062–2072.

Walter, T. J., and M. S. Braiman. 1994. Anion-protein interaction during halorhodopsin pumping: halide binding at the protonated Schiff base. *Biochemistry.* 33:1724–1733.

Zimányi, L., L. Keszthelyi, and J. K. Lanyi. 1989. Transient spectroscopy of bacterial rhodopsins with optical multichannel analyser. 1. Comparison of the photocycles of bacteriorhodopsin and halorhodopsin. *Biochemistry.* 28:5165–5172.

Zimányi, L., A. Kulcsár, J. K. Lanyi, D. F. Sears, Jr., and J. Saltiel. 1999. Singular value decomposition with self-modeling applied to determine bacteriorhodopsin intermediate spectra: analysis of simulated data. *Proc. Natl. Acad. Sci. USA.* 96:4408–4413.

Zimányi, L., and J. K. Lanyi. 1993. Deriving the intermediate spectra and photocycle kinetics from time-resolved difference spectra of bacteriorhodopsin: the simpler case of the recombinant D96N protein. *Biophys. J.* 64:240–251.

Zimányi, L., and J. K. Lanyi. 1997. Fourier transform Raman study of retinal isomeric composition and equilibration in halorhodopsin. *J. Phys. Chem. B.* 101:1930–1933.